

Techno-economic viability of silicon-based tandem photovoltaic modules in the United States

Zhengshan J. Yu*, Joe V. Carpenter III and Zachary C. Holman*

Tandem photovoltaic modules with silicon bottom cells offer a promising route to exceed the single-junction photovoltaic efficiency limit and further lower the levelized cost of solar electricity. However, it is unclear whether continued improvements in efficiency will render tandem modules cost-competitive with their two constituent sub-cells, and with silicon technology in particular. Here, we construct a simple and versatile techno-economic model that, for a given balance-of-systems scenario, calculates the tandem module efficiency and cost from assumed sub-cell module efficiencies and costs. To understand which input conditions are likely to be representative of the future photovoltaic market, we calculate learning rates for both module and area-related balance-of-system costs, and find that the slower learning rate of the latter means that high-efficiency tandems will become increasingly attractive. Further, in the residential market in 2020, the model indicates that top-cell modules could cost up to US\$100 m⁻²—over twice that of the projected silicon module cost—and the associated tandem module would be cost-competitive if its energy yield, degradation rate, service life and financing terms are similar to those of silicon.

In the United States, the levelized cost of electricity (LCOE) generated by photovoltaic modules in an average utility-scale system in an average climate dropped from \$0.27 kWh⁻¹ (we use US\$ throughout) in 2010 to \$0.07 kWh⁻¹ in 2016—without the investment tax credit—as the cumulative photovoltaic capacity installed in the United States skyrocketed from 435 MW to 25 GW^{1,2}. This market growth and electricity cost decline has been driven largely by the rapid fall in the global price for a silicon photovoltaic module: over the same period, the average US module price decreased by 84%. The balance-of-system (BOS) cost—especially the area-related BOS cost, BOS_A—has not fallen as quickly, however, and now accounts for most of the cost of a photovoltaic system^{2,3}. For example, photovoltaic modules accounted for only 34% of the average total utility-scale system cost in 2016, and this fraction is even lower in area-constrained markets such as the residential and commercial markets.

In addition to economies of scale, technological innovation has played a key part in reducing module cost—and thus system cost—and will continue to do so. In particular, higher module efficiency enabled by new cell and module technologies decreases both module costs and BOS_A on a \$ W⁻¹ basis by increasing the system power output. Aluminium back-surface field cell manufacturing lines are at present being upgraded to the passivated emitter and rear contact cell technology, with the best cell efficiencies now exceeding 22%⁴, and routes have been demonstrated to mass-manufactured cells with efficiencies in excess of 25% using heterojunction or interdigitated-back-contact structures⁵. Recently, a silicon cell with 26.6% efficiency was reported, which approaches the 29.4% theoretical efficiency limit for a silicon cell and is on par with the practical efficiency limit of 27%⁶.

As silicon cells and modules approach their terminal efficiency, what will come next for photovoltaic systems? Silicon-based tandems, in which a wide-bandgap top cell is coupled with a silicon bottom cell, are a natural evolutionary step for silicon cells that have the potential to exceed the single-junction efficiency limit. In theory, the limiting one-Sun efficiency of a silicon-based tandem with a 1.7-eV top cell is 43% after taking into account Auger recombination in the silicon bottom

cell⁷. In practice, top cells with III–V and perovskite absorbers have been paired with silicon cells in a range of coupling configurations and have achieved encouraging efficiencies in laboratory-scale devices^{8–12}. For example, with III–V materials, efficiencies of up to 32.8% were reported recently¹⁰, and with perovskites, the record tandem efficiency has increased from 13% to 26% within just three years¹³. As the research efforts show no sign of slowing, it is plausible that these tandems will approach their limiting efficiencies, just as their sub-cells have.

It is not clear, however, whether continued improvements in efficiency are sufficient to propel tandems beyond their constituent sub-cells in terms of cost competitiveness. Peters et al. argued that, for tandems to be cost-competitive, modules composed of their sub-cells should have similar cost—on a \$ W⁻¹ basis—at the system level¹⁴. In other words, a tandem module with expensive top cells and cheap bottom cells would lose out to the corresponding ‘bottom-cell module’ that could be made using the bottom cells alone. After considering present BOS costs, III–V cell costs, and silicon cell costs, Bobela et al. found that a hypothetical III–V/silicon tandem would never offer a cost advantage over both single-junction alternatives¹⁵. Conversely, studies by Werner et al. indicated that perovskite/silicon tandems could be competitive in Europe under specific circumstances¹³. A comprehensive analysis is, however, lacking, and critical questions remain. For instance, under what conditions, if any, could silicon-based tandems compete in the (flat-plate) photovoltaic market? And is there any overlap between those favourable conditions and the projected evolution of the market?

To answer these questions, we constructed a simple and versatile analytical model to compute costs on a system level. Starting with module and BOS inputs, the model returns system costs on a \$ W⁻¹ basis. Although solar project decisions are made based on the projected LCOE, a \$ W⁻¹ analysis is most helpful at this early point in tandem technology development, as data on module degradation rate and energy yield—which are essential for LCOE calculations—are not yet available. We use the model to evaluate the expected maximum competitive cost, or ‘break-even’ cost, of tandem modules in the United States in 2020. The same analysis can be repeated for any location, but the United States was chosen because

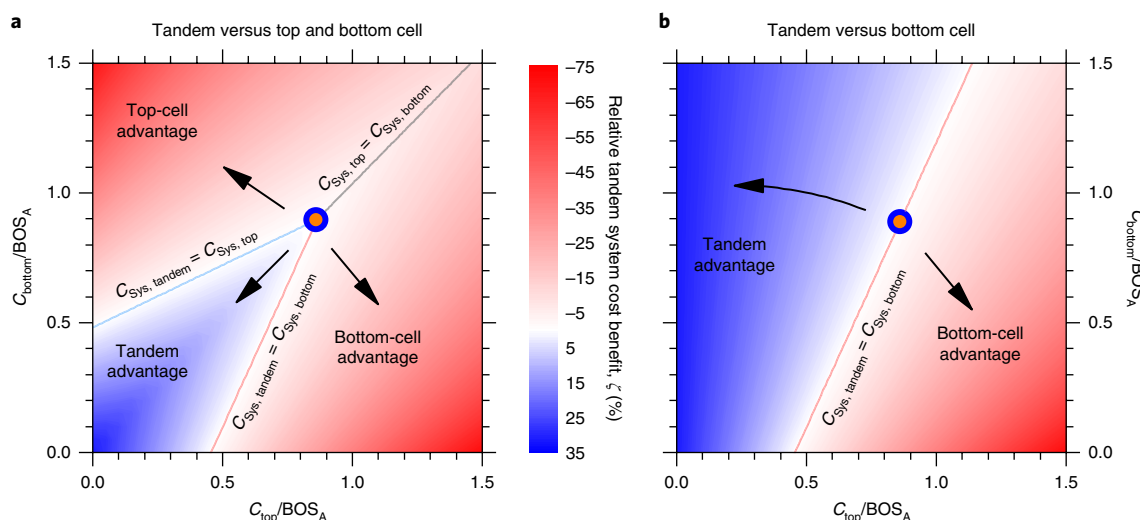


Fig. 1 | Tandem system cost competitiveness plots. **a**, A tandem compared to both of its sub-cells. **b**, A tandem compared to only its bottom cell. The assumed tandem comprises a 1.7-eV, 21.7% efficiency top cell and a 22.1% efficiency silicon bottom cell, resulting in a tandem efficiency of 32.1%. In the blue region, the tandem system has the cost advantage, whereas one of its constituent single-junction sub-cell systems is preferred in the red regions. The blue, red and grey lines mark the iso-cost boundaries of the tandem/top-cell systems, tandem/bottom-cell systems, and top-cell/bottom-cell systems, respectively. The blue and orange circle marks the triple point, at which the tandem, top cell and bottom cell all have the same system cost. The system cost, C_{sys} , is calculated using equation 1 in the Methods, and the relative tandem system cost benefit, ζ , is calculated using equations 4 and 8 for **a** and **b**, respectively.

it is a steadily growing market that represented 20% of installations worldwide in 2016¹⁶, and that has a relatively long history of the reliable and accessible data needed for cost projections. The results provide the target tandem module costs that must be achieved (prior to taking into account the energy yield, reliability, and financing specific to each module and location) to enable emerging tandems to be cost competitive.

Cost competitiveness plots

Peters et al.¹⁴ previously introduced simple plots to visualize the cost competitiveness of tandems. The x and y axes of these plots are the ratio of the constituent single-junction module costs to the 'structural' BOS_A cost, and colour contours show the cost benefit of the tandem relative to the cheaper of the two single-junction modules. Figure 1a shows such a plot constructed using equations 1–4 of our cost model outlined in the Methods. However, the axes were changed to the ratios of sub-cell module areal cost (C_{top} or C_{bottom} , in $\$ m^{-2}$) to BOS_A , as these explicitly scale with area (some costs that scale with power were included in the axes of Peters et al.¹⁴). As explored in detail later, these cost competitiveness plots assume power conversion efficiencies for each sub-cell module, as well as a coupling efficiency with which those modules are married. Figure 1a corresponds to a 1.7-eV, 21.7% efficiency top-cell module coupled losslessly with a 22.1% efficiency silicon bottom-cell module, which yields a 32.1% efficiency tandem module.

The three iso-cost lines in Fig. 1a, defined by equations 5–7 in the Methods, intersect at the 'triple point', which is a convenient anchor in the parameter space. To the upper left of the triple point, the top-cell system has the cost advantage; to the lower right, the bottom-cell system has the advantage; and, to the lower left, the tandem system has the advantage. That is, for the efficiency assumptions in Fig. 1a, this analysis indicates that a tandem would make economic sense only when both sub-cell modules are cheap relative to BOS_A . For example, for a tandem system to have a 10% relative cost benefit over the cheaper of the two sub-cell systems, both the top- and bottom-cell module costs should be less than half of BOS_A . The relative tandem system cost benefit peaks at 31% when both sub-cell modules are free, and diminishes towards the triple point

as well as towards the iso-cost boundaries. We note that the maximum benefit depends only on the efficiencies of the three modules, and not on their absolute costs (as it occurs when their costs go to zero) or on BOS_A . In fact, the maximum cost benefit is identical to the relative tandem efficiency advantage. We also note that a large cost benefit will not necessarily be needed to prefer tandem systems over single-junction systems, because higher efficiencies bring additional perceived benefits such as reduced installation area. It is, however, necessary that the path leading to such a tandem be continuously profitable.

Figure 1a suggests that a module comprising excellent single-junction top cells (small values of C_{top}/BOS_A) would probably beat out both silicon and its associated tandem. However, no new absorber technology has been successful in competing against silicon, which now has approximately 80 GW of momentum and exerts extreme price pressure that is most keenly felt by newcomers to the market. For example, thin-film photovoltaic technologies such as copper indium gallium selenide (CIGS) and cadmium telluride (CdTe) have lost market share—from 17% in 2009 to 6% in 2016¹⁷. Similarly, thin-film silicon and its 'Micromorph' tandem technology were nearly forced out of the market over the last six years as the efficiency of these modules stagnated and the price of crystalline silicon modules dropped¹⁸. Most companies pursuing (concentrating) III–V terrestrial technologies have faced a similar end^{19,20}. In short, silicon photovoltaic technology has proved itself to be difficult to displace.

Silicon module manufacturers also feel the price pressure they collectively create. They are currently struggling with low margins because the global module selling price is close to or even below the module manufacturing cost²¹. For these manufacturers to progress down the learning curve and reduce the selling price of their products while remaining profitable (or at least in business), they must decrease the $\$ W^{-1}$ cost of their modules. As most of the margin has been squeezed out of the raw materials (which account for the majority of the manufacturing cost)^{3,22}, their most promising route is to increase wattage through efficiency gains. We therefore believe that silicon-based tandem technologies will be adopted first by vertically integrated silicon photovoltaic manufacturers seeking to save

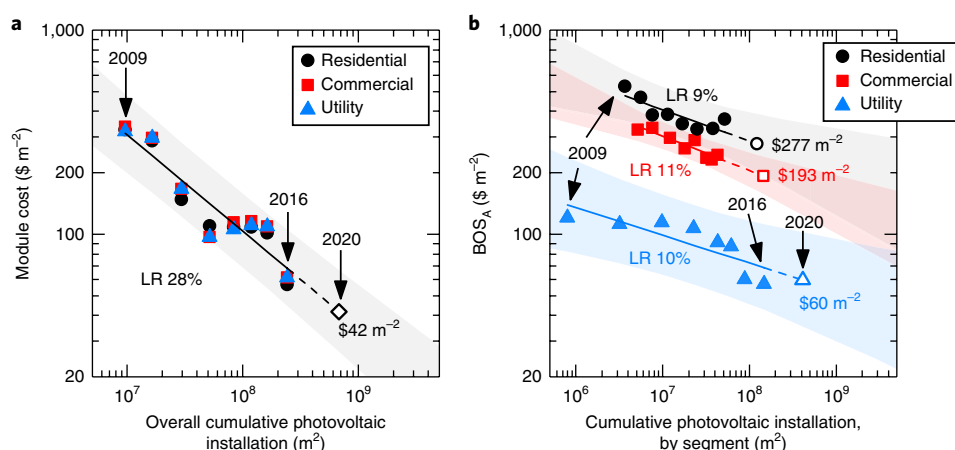


Fig. 2 | Photovoltaic system learning curves. a, Silicon module learning. **b,** Area-related balance-of-systems learning. Cost data (solid symbols) were reported by NREL for installations in the United States². Lines are power-law learning curves fitted to the data and are accompanied by learning rates (LR). Open symbols represent values predicted for 2020. The shaded areas represent the 95% prediction intervals for the future values based on the historical data. Reported annual $\$ W^{-1}$ costs were converted into areal costs using the reported average module efficiency in each year. The cumulative installed photovoltaic area is the sum of the annual installed photovoltaic areas, which were calculated based on the reported annual installation in watts and the average module efficiency in each year.

costs at the system level via module efficiency enhancements. If so, tandem modules will enter the market as an evolution of silicon technology and they will compete with their silicon predecessors—passivated emitter and rear contact modules and interdigitated-back-contact modules, for example—and not with yet-to-be-created single-junction top-cell modules. Figure 1b shows the corresponding tandem system cost competitiveness plot, in which the tandem cost benefit is calculated relative to only the silicon single-junction modules, using equation 8 in the Methods. Though we expect Fig. 1b to be most representative of the competitive landscape, for completeness we nevertheless consider both bottom- and top-cell modules as competitors, below.

Market evolution

As evidenced by the axes in Fig. 1, the ratios of the areal module cost to BOS_A for the top- and bottom-cell modules determine the economic viability of tandems. Although future top-cell module costs are uncertain, the trajectories of the bottom-cell module cost and BOS_A can be accurately estimated for some geographical regions (all analyses up to this point have been independent of location and market). To investigate whether the US flat-plate photovoltaic market is evolving towards or away from conditions that favour tandems, we constructed one-factor learning curves of both average silicon areal module cost and average BOS_A , as shown in Fig. 2, with historical data for US photovoltaic installations reported by NREL².

Figure 2a is an unconventional way to show module learning curves—most are displayed on a $\$ W^{-1}$ basis—but is sensible because module manufacturing costs scale with area and equations 1 and 2 take $\$ m^{-2}$ inputs. Similar or identical silicon modules are used on rooftops and in solar power plants, and thus we used cumulative US photovoltaic installation as the metric of experience (the x axis); this also explains why module costs do not vary appreciably across market segments. In contrast, the racking for modules on tiled home roofs differs from that on flat commercial roofs, which differs from that on the desert ground. That is, area-related BOS components are mostly—but not exclusively—particular to the installation type, and thus we used cumulative photovoltaic installation by market segment as the metric of experience in Fig. 2b. The learning rates decrease (most for residential and very little for utility) if BOS_A experience is instead assumed not to be segmented. We also note that the BOS components that are included in BOS_A are different for the different market segments, as proposed by Bobela et al¹⁵.

In particular, for the utility market, BOS_A includes BOS equipment, installation labour and land, whereas for the (area-constrained) residential and commercial markets, BOS_A also includes permits, inspection and interconnection; installer overhead and profit; and sales tax (that is, all BOS components except inverters).

Figure 2a shows that the silicon module cost decreased from $\$320 m^{-2}$ in 2009 to $\$60 m^{-2}$ in 2016. Fitting the historical data with a power-law learning curve using the least-squares method, we find a learning rate of 28%, which means that the areal module cost has decreased by 28% for every doubling of the cumulative photovoltaic area installed. The International Technology Roadmap for Photovoltaic reported a comparable, 26.2% per-piece learning rate on a global basis²³. Figure 2b shows that BOS_A for the utility market decreased from $\$120 m^{-2}$ in 2009 to $\$57 m^{-2}$ in 2016, resulting in a learning rate of only 10%. The learning rates are similar for the residential and commercial markets, though there have been fewer installations and the absolute BOS_A is higher. The three-fold discrepancy between the module and BOS_A learning rates helps to explain the market push towards higher module efficiencies in the past decade and the disappearance of cheap but inefficient modules, like those of thin-film silicon ($\$70 m^{-2}$ and $<10\%$ efficiency in 2011)²⁴. More importantly, if these learning rates are sustained, tandems will continue to become increasingly attractive in the market: since 2009, C_{bottom}/BOS_A has fallen by a factor of 2.5 for the utility market and approximately 4 for the commercial and residential markets.

We next projected out to 2020—not because market-ready tandem technologies will be available by that year, but because increasing uncertainty renders more distant projections unproductive. We first calculated the expected areal annual photovoltaic installation in the United States using the annual forecast (in watts) by SEIA and GTM Research²⁵ and the compound annual growth rate of module efficiency extracted from NREL data². Extension of the learning curves to the appropriate installation areas then yields the open symbols in Fig. 2: in 2020, the areal silicon module cost will be $\$42 m^{-2}$ and BOS_A will be $\$277 m^{-2}$, $\$193 m^{-2}$, and $\$60 m^{-2}$ for the residential, commercial and utility markets, respectively. Note that the 2020 projected utility BOS_A is higher than its current value—it is not yet clear if the present cost is an aberration and a correction will occur or if there has been a true shift off the historical learning curve. To visualize such uncertainties in the projected values, Fig. 2 also shows the 95% prediction intervals (shaded areas), which account

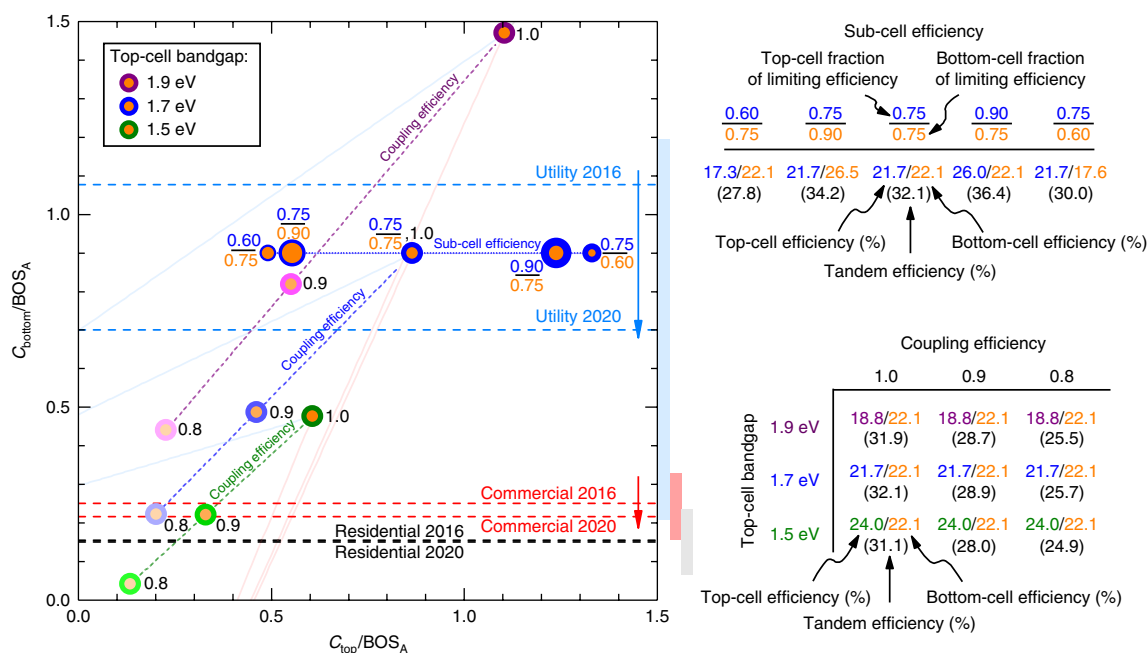


Fig. 3 | Competitive landscape for tandem systems. Tandem system cost competitiveness plot with perturbations in top-cell bandgap, sub-cell efficiency and coupling efficiency. Dashed horizontal lines are actual (2016) and predicted (2020) ratios of silicon areal module cost to BOS_A , with data from Fig. 2, and the shaded blue, red and grey vertical strips to the right represent the 95% prediction intervals of the 2020 values. The ratios accompanying the blue and orange triple points indicate the efficiencies of the constituent 1.7-eV top cell and silicon bottom cell relative to their respective limiting efficiencies (triple points without ratios all have the default ratio of 0.75/0.75). This information is also indicated qualitatively by the relative size of the blue and orange areas of the triple points. The absolute efficiencies of these sub-cells, as well as their tandems, appears in the table in the upper right. The colour of the outer ring of the triple points corresponds to the top-cell bandgap, as indicated. The saturation of the colours reflects the coupling efficiency, which is also indicated next to the triple points with a value between 0.8 and 1.0 (triple points without such numbers all have the default value of 1.0). The table in the lower right shows the sub-cell and tandem absolute efficiencies associated with these variations in top-cell bandgap and coupling efficiency.

for both the error in the fit based on the existing observations and the random error in the projected BOS_A value²⁶. According to this analysis, C_{bottom}/BOS_A is expected to fall to 0.15, 0.22 and 0.70 in the residential, commercial and utility markets, respectively, which is up to 1.5 times lower than in 2016.

Tandem opportunity

Given these projected values, how expensive and inefficient can the top-cell module be in 2020 and still yield a cost-competitive tandem? Figure 3 is a tandem system cost competitiveness plot overlaid with the 2016 and projected 2020 values for C_{bottom}/BOS_A , which appear as horizontal lines. The shaded strips to the right of the plot represent the propagated uncertainty from the 95% prediction intervals of the 2020 module and BOS_A values taken from Fig. 2. As a rule of thumb, if a tandem is to be cost competitive against both its corresponding top- and bottom-cell modules, its triple point must be above the C_{bottom}/BOS_A line. Also, for tandems to be competitive over only the silicon bottom-cell module, the top-cell module has to be cheaper than the C_{top} value associated with the point at which the (light-red) tandem–silicon iso-cost line intersects the C_{bottom}/BOS_A line.

For example, consider again the blue and orange triple point of the 32.1% efficiency tandem shown in Fig. 1, which now appears in the middle of Fig. 3 with the label '0.75/0.75, 1.0'. This notation indicates that both sub-cells operate at 75% of their respective limiting efficiencies—as mature manufactured photovoltaic technologies do—and are coupled with unity efficiency (these quantities, along with the top-cell bandgap, provide enough information to use equation 3). The triple point for this tandem is below the 'Utility 2016' line ($C_{\text{bottom}} = \$60 \text{ m}^{-2}$, $BOS_A = \$57 \text{ m}^{-2}$ and $C_{\text{bottom}}/BOS_A = 1.07$) but above the 'Utility 2020' line ($C_{\text{bottom}} = \$42 \text{ m}^{-2}$, $BOS_A = \$60 \text{ m}^{-2}$ and $C_{\text{bottom}}/BOS_A = 0.70$). Consequently, in 2016, the tandem system

could have beaten only the silicon bottom-cell system (never the top-cell system), and only if the 21.7% efficiency top-cell module had cost less than $\$53 \text{ m}^{-2}$. In contrast, in 2020, the tandem will be cost competitive against both single junctions if the top-cell module costs between $\$27 \text{ m}^{-2}$ and $\$46 \text{ m}^{-2}$. If the top-cell module is less than $\$27 \text{ m}^{-2}$, the tandem will lose to the top-cell system; if the top-cell module is greater than $\$46 \text{ m}^{-2}$, the tandem will lose to the bottom-cell system. Even if the utility BOS_A falls to $\$35 \text{ m}^{-2}$ at the most aggressive edge of the 2020 prediction interval, Fig. 3 shows that tandems will be nearly as competitive as they were in the utility market in 2016 (uppermost edge of blue shaded strip), and in all other BOS_A scenarios they will be considerably more competitive.

Similarly, in 2020, the top-cell module break-even cost for the commercial market ($C_{\text{bottom}} = \$42 \text{ m}^{-2}$, $BOS_A = \$193 \text{ m}^{-2}$ and $C_{\text{bottom}}/BOS_A = 0.22$) will be $\$107 \text{ m}^{-2}$, whereas for the residential market ($C_{\text{bottom}} = \$42 \text{ m}^{-2}$, $BOS_A = \$277 \text{ m}^{-2}$ and $C_{\text{bottom}}/BOS_A = 0.15$) it will be $\$145 \text{ m}^{-2}$. 'Break-even cost' is used here to mean the top-cell module cost or tandem module cost—as specified—at which a tandem system reaches cost parity with a system comprising silicon bottom-cell modules. These values are considerably higher than the current areal costs of silicon or thin-film modules, giving appreciable margin for development of these new technologies. Also, the C_{bottom}/BOS_A lines do not intersect the tandem–top-cell iso-cost line for these markets, indicating that silicon will be the only competitor for tandems, even if our earlier price-pressure argument proves false. High- BOS_A residential and commercial systems thus appear to form a favourable entry market for silicon-based tandems; however, these markets have not historically driven photovoltaic innovation because the end customers are insufficiently educated to demand the highest-performance modules. The key to successful introduction of tandems will thus be strong partnerships between module manufacturers and

installers who understand that they can offer lower system prices with higher-efficiency modules, or vertical integration between module manufacturers and installers. SunPower, with its premium interdigitated-back-contact modules, provides a model for the former route, and the Tesla/Panasonic partnership for the latter.

The '0.75/0.75, 1.0' cell in Fig. 3 represents just one of the many possible future tandems, and the performance of its assumed top cell (21.7% efficiency, 1.7 eV) has not yet been realized. The best reported 1.7-eV top cell, achieved with a perovskite absorber, has an efficiency of approximately 17%²⁷. If a 17.3% efficiency, 1.7-eV top cell (60% of its limiting efficiency) is coupled losslessly with the 22.1% efficiency silicon bottom cell (still 75% of its limiting efficiency), the expected tandem efficiency is only 27.8%. As a result, the triple point, labelled '0.60/0.75' in Fig. 3, moves leftward: the tandem cost-advantage region diminishes, whereas the bottom-cell cost-advantage region increases. This 13% relative decrease in tandem efficiency compared to the '0.75/0.75, 1.0' tandem causes an outsized effect on cost competitiveness, as the top-cell module break-even cost diminishes by 43%, regardless of the market (C_{bottom}/BOS_A). On the other hand, if the 1.7-eV top cell reaches 26.0% (90% of its limiting efficiency), the tandem is 36.4% efficient, the triple point, labelled '0.90/0.75', moves rightward, and the top-cell module break-even cost increases by 43%. A similar efficiency perturbation of the silicon bottom cell—refer to the points labelled '0.75/0.90' and '0.75/0.60'—produces similar outcomes.

1.7 eV is the ideal bandgap for a top cell paired with an ideal silicon cell in a two-terminal tandem owing to the current-matching constraint⁷. Four- and three-terminal configurations, however, remove the constraint and can thus tolerate a wider range of bandgaps with minimal sacrifice in tandem efficiency^{28,29}. Varying the bandgap of the top cell changes the efficiency contributions from the top and bottom cells to the tandem, and thus the location of the triple point, according to equations 5–7. This is apparent in Fig. 3, which displays data for top cells with three bandgaps, all of which operate at 75% of their limiting efficiencies and are paired with the previous 22.1% efficiency silicon cell. Increasing the bandgap of the top cell lifts the triple point (purple and orange point labelled '1.0' near the top of the plot), whereas decreasing the bandgap lowers it (green and orange point labelled '1.0'). However, the bottom-cell cost-advantage region remains similar in all cases, indicating that the top-cell bandgap does not affect competitiveness with incumbent silicon technologies. Rather, it trades tandem cost-advantage territory only with top-cell territory. As shown in the first column of the coupling efficiency table in Fig. 3, the 18.8% efficiency, 1.9-eV top cell yields a 31.9% efficiency tandem. Its triple point is above even the 'Utility 2016' line, which means that this tandem system has the largest opportunity to be cost effective compared to both of its sub-cell systems. Recall, however, that no matter how far out the triple point of a given system, the largest tandem cost benefit always occurs for C_{bottom} , C_{top} , and BOS_A combinations near the origin.

In addition to varying sub-cell efficiency and bandgap, tandem photovoltaic researchers can engineer how sub-cells are coupled. The coupling efficiency of the best reported tandem devices ranges from 0.7 to close to unity (see Supplementary Fig. 2), with the majority over 0.9 and thus encouragingly close to the ideal value heretofore assumed. This is important, as decreasing the coupling efficiency proportionally dampens the tandem efficiency (equation 3) and thus shifts the triple point undesirably towards the origin. For example, as displayed in the coupling efficiency table in Fig. 3, the efficiency of tandems decreases from 31–32% to 28–29% and then to 25–26% as the coupling efficiency is reduced to 0.9 and then to 0.8, and the top-cell module break-even cost shrinks by approximately one-third each time.

Figure 4 summarizes the projected 2020 tandem module break-even cost for the range of markets, coupling efficiencies and top-cell bandgaps explored in Fig. 3. The tandem (and top-cell) module

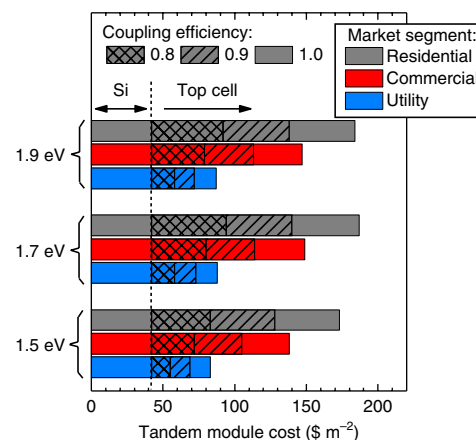


Fig. 4 | Allowable tandem module cost. Maximum tandem module cost to reach system capital cost parity with a silicon system in 2020 for various US markets, coupling efficiencies, and top-cell bandgaps. All cases assume that both sub-cells operate at 75% of their limiting efficiencies (0.75/0.75).

break-even costs are very similar for different top-cell bandgaps, but they depend strongly on the market and coupling efficiency. As coupling efficiencies of 0.9 are realistic, top-cell modules can cost up to approximately \$100 m⁻², \$70 m⁻², and \$30 m⁻² and probably still generate competitive tandems in the 2020 residential, commercial and utility markets, respectively. (Of course, this presumes that their non-capital LCOE cost drivers, including energy yield and reliability, can be made comparable to those of silicon.) With the projected cost of silicon modules at \$42 m⁻² in the same year, the top-cell module cost targets for the two area-constrained markets seem like they may be achievable and justify continued research and development of top-cell technologies. The target for the utility market, however, is quite aggressive and thus power plants are unlikely to be the market entry point for tandems.

Conclusions

The analysis presented here predicts that silicon-based tandem photovoltaic modules will become increasingly attractive in the United States because of the disparity in the silicon module and area-related balance-of-system learning rates. Tandems are expected to compete only with the incumbent single-junction silicon modules, and are most likely to enter area-constrained markets through vertically integrated silicon module and system manufacturers seeking product differentiation. The critical challenge to realizing this future is the demonstration of a wide-bandgap photovoltaic technology with an efficiency above approximately 20%, an areal cost below \$100 m⁻², the ability to be integrated with silicon photovoltaic cells with little coupling loss (in at least a four-terminal configuration), and sufficient durability to justify 25-year warranties.

There are several opportunities to learn more from this analytical cost model. The present analysis considered only US data, and, while module costs are similar worldwide, BOS costs (especially BOS_A) vary dramatically. With appropriate data, it would be valuable to recreate Fig. 4 for important markets like China, Japan and India to investigate whether particular geographical areas are more likely to adopt tandems than others. The analysis also treated only power densities, assuming an AM1.5 G spectrum, and extension to an energy analysis that compared tandem and sub-cell LCOE would better reflect cost installation drivers. As a first step that still ignores financing and reliability, this can be conveniently accomplished by adapting only equation 3 to account for the spectral variation in a given location, and the spectral efficiency formulation naturally lends itself to this. Such an investigation will begin to separate two-terminal from four-terminal tandem configurations, as the coupling

efficiency on an energy basis of the former should be lower in outdoor conditions³⁰. Finally, although this analysis focused on silicon bottom cells, it is trivial to probe other sub-cell combinations—for example, II–VI/CIGS³¹, perovskite/CIGS³², or perovskite/perovskite³³—by using the appropriate inputs in equations 2 and 3.

Methods

Cost model. The capital cost of a photovoltaic system (C_{system}), in \$ W⁻¹, is given by

$$C_{\text{system}} \left[\frac{\$}{\text{W}} \right] = \frac{C_{\text{module}} \left[\frac{\$}{\text{m}^2} \right]}{\eta \cdot 1,000 \left[\frac{\text{W}}{\text{m}^2} \right]} + \frac{\text{BOS}_A \left[\frac{\$}{\text{m}^2} \right]}{\eta \cdot 1,000 \left[\frac{\text{W}}{\text{m}^2} \right]} + \text{BOS}_P \left[\frac{\$}{\text{W}} \right] \quad (1)$$

where C_{module} is the areal module cost to the system owner, η is the module efficiency, BOS_P is the power-related BOS cost, and the units of each quantity are given in square brackets. This model can be applied to any type of photovoltaic system (residential, commercial or utility) by varying the BOS_A and BOS_P input values, and to any type of photovoltaic module by varying the C_{module} and η inputs. In particular, equation 1 can be used to calculate the system cost for an installation with single-junction top-cell modules ($C_{\text{module}} = C_{\text{top}}$) or bottom-cell modules ($C_{\text{module}} = C_{\text{bottom}}$) or with tandem modules ($C_{\text{module}} = C_{\text{tandem}}$).

One way to calculate the cost of a hypothetical tandem module is as a perturbation to the costs of its constituent single-junction modules. Equation 2 does this by summing the top-cell and bottom-cell module costs and subtracting the overlap cost (C_{overlap}):

$$C_{\text{tandem}} = C_{\text{top}} + C_{\text{bottom}} - C_{\text{overlap}} \quad (2)$$

Consistent with equation 1, all costs are in \$ m⁻². The single-junction module costs include all elements of a standard module—cells, glass, encapsulants, frames, junction boxes, and so on—and the overlap costs might include, for example, double-counted encapsulants and glass. However, we assume $C_{\text{overlap}} = 0$ hereafter. As shown in Supplementary Note 1, this turns out to be necessary to ‘orthogonalize’ the contributions of the top-cell and bottom-cell module costs in our model, which simplifies the analysis so that we may draw generally applicable conclusions. Furthermore, while this is a conservative assumption, it is not the worst-case assumption, because tandems can conceivably cost more than the sum of their constituent sub-cells (negative C_{overlap}). For example, two-terminal tandems may require extra processing steps during recombination-junction formation, and four-terminal tandems may require extra layers or spectrum-splitting designs for optimal optical coupling.

Equation 1 converts areal costs into power costs by dividing by module output power density, which is the product of module efficiency and the AM1.5G 1,000 W m⁻² input power density. Thus, we also need to calculate the tandem module efficiency (η_{tandem}), given by

$$\eta_{\text{tandem}} = (\eta_{\text{top}} + f \cdot \eta_{\text{bottom}}) \cdot \eta_{\text{coupling}} \quad (3)$$

In equation 3, η_{top} is the efficiency of the top-cell module, η_{bottom} is the efficiency of the bottom-cell module (both measured alone, under AM1.5G illumination), f is the fraction of η_{bottom} that contributes to the tandem efficiency in the absence of coupling losses, and η_{coupling} is the coupling efficiency of the sub-cell modules in the tandem. Equation 3 is a simplification of the spectral-efficiency-based tandem coupling model we introduced previously⁷. That model expresses the efficiency of a tandem in which a silicon cell and a hypothetical top cell operating at a fraction of its detailed-balance limit are coupled, and it includes ‘spectral fidelity’ terms that describe how much light at each wavelength reaches the top and bottom cells. To arrive at equation 3, we first assumed ideal spectral fidelities. This means that all photons with energies below the top-cell bandgap energy reach the bottom cell, and thus f is a function only of the bandgap of the top cell. (f values can be found in Supplementary Fig. 1) We then re-introduced optical losses within the η_{coupling} catch-all term, which also includes any electrical losses (or gains) and can be assigned an arbitrary value in accordance with the relative success of the tandem assembly process. We note that, unlike a detailed-balance model, equation 3 can calculate the efficiency of a tandem comprising realistic, imperfect sub-cells. For example, consider a 1.7-eV, 21.7% efficiency top-cell module and a 22.1% efficiency silicon module, as in Fig. 1. From Supplementary Fig. 1, $f = 0.473$ and thus the silicon module can contribute 10.4% absolute efficiency to the tandem, assuming unity η_{coupling} , resulting in a 32.1% efficiency tandem module.

In Fig. 1a, the relative tandem system cost benefit, ζ , is calculated using equation 4, with each system capital cost calculated using equation 1.

$$\zeta = \frac{\min(C_{\text{system,top}}, C_{\text{system,bottom}}) - C_{\text{system,tandem}}}{\min(C_{\text{system,top}}, C_{\text{system,bottom}})} \quad (4)$$

BOS_P is independent of module type and was set to zero (in equation 1) throughout this study in order to visualize the maximum possible cost benefits

and detriments. Non-zero BOS_P values do not change the sign of the cost benefit but just reduce its absolute value. For example, with $\text{BOS}_P = \$0.06 \text{ W}^{-1}$ —a typical inverter cost—the maximum cost benefit in Fig. 1a reduces from 31% to 29%.

Equations 5, 6 and 7 express, respectively, the conditions for which the tandem system cost equals the bottom-cell system cost, the tandem system cost equals the top-cell system cost, and the top-cell system cost equals the bottom-cell system cost. (Derivations can be found in Supplementary Note 1.) The associated iso-cost lines are shown in Fig. 1a.

$$\frac{C_{\text{top}}}{\text{BOS}_A} \cdot \eta_{\text{bottom}} = (\eta_{\text{tandem}} - \eta_{\text{bottom}}) \cdot \left(\frac{C_{\text{bottom}}}{\text{BOS}_A} + 1 \right) \quad (5)$$

$$\frac{C_{\text{bottom}}}{\text{BOS}_A} \cdot \eta_{\text{top}} = (\eta_{\text{tandem}} - \eta_{\text{top}}) \cdot \left(\frac{C_{\text{top}}}{\text{BOS}_A} + 1 \right) \quad (6)$$

$$\left(\frac{C_{\text{top}}}{\text{BOS}_A} + 1 \right) \cdot \eta_{\text{bottom}} = \left(\frac{C_{\text{bottom}}}{\text{BOS}_A} + 1 \right) \cdot \eta_{\text{top}} \quad (7)$$

In Fig. 1b, which compares the tandem to the silicon bottom cell alone, the relative system cost benefit expressed in equation 4 is instead calculated as

$$\zeta = \frac{C_{\text{system,bottom}} - C_{\text{system,tandem}}}{C_{\text{system,bottom}}} \quad (8)$$

Data availability. The data that support the plots within this paper and other findings of this study are available from the corresponding authors upon reasonable request.

Received: 6 January 2018; Accepted: 11 June 2018;

Published online: 30 July 2018

References

- Cole, W. J. et al. *SunShot 2030 for Photovoltaics (PV): Envisioning a Low-cost PV Future* (National Renewable Energy Laboratory, 2017); <https://doi.org/10.2172/1392206>
- Fu, R., Feldman, D. J., Margolis, R. M., Woodhouse, M. A. & Ardani, K. B. *US Solar Photovoltaic System Cost Benchmark: Q1 2017* (National Renewable Energy Laboratory, 2017); <https://www.nrel.gov/docs/fy17osti/68925.pdf>
- Woodhouse, M. et al. *On the Path to SunShot. The Role of Advancements in Solar Photovoltaic Efficiency, Reliability, and Costs* Report No. NREL/TP--6A20-65872 United States 10.2172/1253983 (National Renewable Energy Laboratory, 2016); <https://www.nrel.gov/docs/fy16osti/65872.pdf>
- Ye, F. et al. in *2016 IEEE 43rd Photovoltaic Specialists Conference (IEEE, 2016)*; <https://doi.org/10.1109/PVSC.2016.7750289>
- Green, M. A. et al. Solar cell efficiency tables (version 50). *Progr. Photovolt.* **25**, 668–676 (2017).
- Yoshikawa, K. et al. Silicon heterojunction solar cell with interdigitated back contacts for a photoconversion efficiency over 26%. *Nat. Energy* **2**, 17032 (2017).
- Yu, Z., Leilaouioun, M., & Holman, Z. Selecting tandem partners for silicon solar cells. *Nat. Energy* **1**, 16137 (2016).
- Grassman, T. J., Chmielewski, D. J., Carnevale, S. D., Carlin, J. A. & Ringel, S. A. GaAs_{0.75}P_{0.25}/Si dual-junction solar cells grown by MBE and MOCVD. *IEEE J. Photovolt.* **6**, 326–331 (2016).
- Cariou, R. et al. Monolithic two-terminal III–V/Si triple-junction solar cells with 30.2% efficiency under 1-Sun AM1.5g. *IEEE J. Photovolt.* **7**, 367–373 (2017).
- Essig, S. et al. Raising the one-sun conversion efficiency of III–V/Si solar cells to 32.8% for two junctions and 35.9% for three junctions. *Nat. Energy* **2**, 17144 (2017).
- Bush, K. A. et al. 23.6%-efficient monolithic perovskite/silicon tandem solar cells with improved stability. *Nat. Energy* **2**, 17003 (2017).
- Duong, T. et al. Rubidium multication perovskite with optimized bandgap for perovskite-silicon tandem with over 26% efficiency. *Adv. Energy Mater.* **7**, 1700228 (2017).
- Werner, J., Niesen, B. & Ballif, C. Perovskite/silicon tandem solar cells: marriage of convenience or true love story? – An overview. *Adv. Mater. Interf.* **5**, 1700731 (2017).
- Peters, I. M., Sofia, S., Mailoa, J. & Buonassisi, T. Techno-economic analysis of tandem photovoltaic systems. *RSC Adv.* **6**, 66911–66923 (2016).
- Bobela, D. C., Gedvilas, L., Woodhouse, M., Horowitz, K. A. W. & Basore, P. A. Economic competitiveness of III–V on silicon tandem one-sun photovoltaic solar modules in favorable future scenarios. *Progr. Photovolt.* **10.1002/pip.2808** **25**, 41–48 (2016).

16. A *Snapshot of Global PV (1992–2016)* (Photovoltaic Power Systems Programme, International Energy Agency, 2017); http://www.iea-pvps.org/fileadmin/dam/public/report/statistics/IEA-PVPS_-_A_Snapshot_of_Global_PV_-_1992-2016__1_.pdf
17. *Photovoltaics Report* (Fraunhofer ISE, 2017); <https://www.ise.fraunhofer.de/en/publications/studies/photovoltaics-report.html>
18. Wesoff, E. *The End of Oerlikon's Amorphous Silicon Solar Saga* (GreenTechMedia, 2014); <https://www.greentechmedia.com/articles/read/the-end-of-oerlikons-amorphous-silicon-solar-saga>.
19. Wesoff, E. *CPV Hopeful Soitec Latest Victim of the Economics of Silicon Photovoltaics* (GreenTechMedia, 2014); <https://www.greentechmedia.com/articles/read/cpv-hopeful-soitec-latest-victim-of-the-economics-of-silicon-photovoltaics>
20. Stefanchich, M., Chiesa, M. & Apostoleris, H. *Do We Still Care About CPV?* (International Society for Optics and Photonics, 2017); <https://doi.org/10.1117/12.2273701>.
21. *Photovoltaic Manufacturer Capacity, Shipments, Price & Revenues* (SPV Market Research, 2017); <http://www.spvmarketresearch.com>
22. Louwen, A., van Sark, W., Schropp, R. & Faaij, A. A cost roadmap for silicon heterojunction solar cells. *Sol. Energ. Mat. Sol. C* **147**, 295–314 (2016).
23. *International Technology Roadmap for Photovoltaic: Results 2016* (ITRPV, 2017); <http://www.itrpv.net/Reports/Downloads/2017/>
24. SolarServer. *Global Solar Industry Website* (accessed December 2016); <https://www.solarserver.com>
25. *Solar Market Insight Report 2017 Q2* (Solar Energy Industries Association/GTM Research, 2017); <https://www.seia.org/research-resources/solar-market-insight-report-2017-q2>
26. Montgomery, D. C., Peck, E. A. & Vining, G. G. *Introduction to Linear Regression Analysis* 5th edn (Wiley, 2013).
27. McMeekin, D. P. et al. A mixed-cation lead mixed-halide perovskite absorber for tandem solar cells. *Science* **351**, 151–155 (2016).
28. Todorov, T., Gunawan, O. & Guha, S. A road towards 25% efficiency and beyond: perovskite tandem solar cells. *Mol. Syst. Des. Eng.* **1**, 370–376 (2016).
29. Warren, Emily L. et al. Maximizing tandem solar cell power extraction using a three-terminal design. *Sustain. Energy Fuels* **2**, 1141–1147 (2018).
30. Liu, H., Aberle, A. G., Buonassisi, T., & Peters, I. M. On the methodology of energy yield assessment for one-Sun tandem solar cells. *Sol. Energy* **135**, 598–604 (2016).
31. Mailoa, J. P. et al. Energy-yield prediction for II–VI-based thin-film tandem solar cells. *Energy Environ. Sci.* **9**, 2644–2653 (2016).
32. Shen, H. et al. Mechanically-stacked perovskite/CIGS tandem solar cells with efficiency of 23.9% and reduced oxygen sensitivity. *Energy Environ. Sci.* **11**, 394–406 (2018).
33. Eperon, G. E. et al. Perovskite-perovskite tandem photovoltaics with optimized band gaps. *Science* **354**, 861–865 (2016).

Acknowledgements

We thank R. Fu (NREL), P. Mints (SPV Market Research), and C. Gay (DOE SETO) for discussions. The information, data and work presented herein were funded in part by the US Department of Energy, Office of Energy Efficiency and Renewable Energy, under Award Number DE-EE0006709, by the National Science Foundation under Award Number 1664669, and by the Engineering Research Center Program of the National Science Foundation and the Office of Energy Efficiency and Renewable Energy of the Department of Energy under NSF Cooperative Agreement Number EEC-1041895.

Author contributions

Z.J.Y. developed the model, performed the analysis, and drafted the manuscript. J.V.C. assisted in data collection. Z.C.H. conceived the project idea and revised the manuscript. All authors approved the manuscript.

Competing interests

The authors declare no competing interests.

Additional information

Supplementary information is available for this paper at <https://doi.org/10.1038/s41560-018-0201-5>.

Reprints and permissions information is available at www.nature.com/reprints.

Correspondence and requests for materials should be addressed to Z.J.Y. or Z.C.H.

Publisher's note: Springer Nature remains neutral with regard to jurisdictional claims in published maps and institutional affiliations.